



Testing CMAQ chemistry sensitivities in base case and emissions control runs at SEARCH and SOS99 surface sites in the southeastern US

J.R. Arnold^{a,*}, Robin L. Dennis^b

^a*Atmospheric Sciences Modeling Division, Air Resources Laboratory, National Oceanic and Atmospheric Administration, in partnership with the National Exposure Research Laboratory, US Environmental Protection Agency, Office of Research and Development, 1200 6th Avenue/9th FL/OEA-095, Seattle, WA 98101-1128 USA*

^b*Mail Drop E243-05, Research Triangle Park, NC 27711, USA*

Received 4 March 2005; received in revised form 28 May 2005; accepted 28 May 2005

Abstract

CMAQ was run to simulate urban and regional tropospheric conditions in the southeastern US over 14 days in July 1999 at 32, 8 and 2 km grid spacings. Runs were made with either of two older mechanisms, Carbon Bond IV (CB4) and the Regional Acid Deposition Model, version 2 (RADM2), and with the more recent and complete California Statewide Air Pollution Research Center, version 1999 mechanism (SAPRC99) in a sensitivity matrix with a full emissions base case and separate 50% control scenarios for emissions of nitrogen oxides (NO_x) and volatile organic compounds (VOC). Results from the base case were compared to observations at the Southeastern Aerosol Research and Characterization Study (SEARCH) site at Jefferson Street in Atlanta, GA (JST) and the Southern Oxidant Study (SOS) Cornelia Fort Airpark (CFA) site downwind of Nashville, TN. In the base case, SAPRC99 predicted more ozone (O_3) than CB4 or RADM2 almost every hour and especially for afternoon maxima at both JST and CFA. Performance of the 8 km models at JST was better than that of the 32 km ones for all chemistries, reducing the 1 h peak bias by as much as 30 percentage points; at CFA only the RADM2 8 km model improved. The 2 km solutions did not show improved performance over the 8 km ones at either site, with normalized 1 h bias in the peak O_3 ranging from 21% at CFA to 43% at JST. In the emissions control cases, SAPRC99 was generally more responsive than CB4 and RADM2 to NO_x and VOC controls, excepting hours at JST with predicted increased O_3 from NO_x control. Differential sensitivity to chemical mechanism varied by more than $\pm 10\%$ for NO_x control at JST and CFA, and in a similar range for VOC control at JST. VOC control at the more strongly NO_x -limited urban CFA site produced a differential sensitivity response of $< 5\%$. However, even when differential sensitivities in control cases were small, neither their sign nor their magnitude could be reliably determined from model performance in the full emissions case, meaning that the degree of O_3 response to a change in chemical mechanism can differ substantially with the level of precursor emissions. Hence we conclude that properly understanding the effects of changes in a model's chemical mechanism always requires emissions control cases as part of model sensitivity analysis.

© 2006 Elsevier Ltd. All rights reserved.

Keywords: Model evaluation; Sensitivity analysis; Chemical mechanism; Emissions control strategies; Differential sensitivity

*Corresponding author. Tel.: +1 206 553 85 79; fax: +1 206 553 8210.

E-mail address: arnold.jeff@epa.gov (J.R. Arnold).

1. Introduction

Uncertainties in key elements of emissions and meteorology inputs to air quality models (AQMs) can range from 50% to 100% with some areas of emissions uncertainty even higher (Russell and Dennis, 2000). Uncertainties in the models' chemical mechanisms are thought to be smaller (Russell and Dennis, 2000), but can range to 30% or more as new techniques are applied to re-measure reaction rate constants and yields. Single perturbation sensitivity analyses have traditionally been used with AQMs to characterize effects of these uncertainties on peak predicted ozone concentration ($[O_3]$). To advance scientific understanding of AQMs so that they may be used with confidence in regulatory applications, however, single perturbation experiments are insufficient. We must also learn more precisely how the physical and chemical dynamics represented in model processes interact to produce model predictions under full emissions base cases and for possible oxides of nitrogen ($NO + N-O_2 = NO_x$) and volatile organic compounds (VOC) precursor control cases. These emissions reduction experiments directly explore the model's relevant O_3 response and are the chief use of the model in regulatory applications where we wish to know both the magnitude of the $[O_3]$ change for planned future emissions changes and whether NO_x or VOC emissions controls are to be preferred. Moreover, for sensitivity analysis, emissions reduction simulations give the true depiction of the photochemical system change. We define this change as the O_3 control response, $\delta O_3/\delta NO_x$ and $\delta O_3/\delta E_{VOC}$, where δNO_x or δE_{VOC} is often termed a control strategy, i.e. the type and amount of precursor emissions control required to reduce O_3 to acceptable levels. The model's most important sensitivity, correspondingly, is how its control response is changed by perturbation of uncertain inputs and parameters in the emissions control cases, not simply how the resultant $[O_3]$ might be changed by uncertainties in a base case full emissions simulation without controls. We define that latter quantity as δO_3 , or the total change in $[O_3]$ in the full emissions case due only to the uncertainty perturbation without controls.

However, producing model simulations with the range of input uncertainties necessary to characterize the $\delta O_3/\delta NO_x$ and $\delta O_3/\delta E_{VOC}$ response for several uncertainties and levels of emissions control has been computationally expensive with large models and can greatly complicate interpretation

of results. For these reasons AQM sensitivity analyses have been focused largely on the first step, characterizing δO_3 , with the assumption that $\delta O_3/\delta NO_x$ and $\delta O_3/\delta E_{VOC}$ will be smaller and can be inferred from the δO_3 sensitivity. We tested this assumption in an earlier, much smaller sensitivity project (Dennis et al., 1999) with a version of another AQM, RADM, and showed that analyzing only δO_3 gives an incomplete and distorted depiction of model behavior for the control strategy response. Briefly put, this distortion results because model resultants like $[O_3]$ are nonunique solutions to the strongly nonlinear equations representing the photochemical system's complex dynamics. That is to say, the complex interaction among the model's multiple chemical pathways as chemical concentrations change over time, and between the chemistry and the meteorology represented in the model, provide multiple ways to produce the same resultant species concentration. All these paths to the resultant concentration can then be altered by the emissions reductions such that the emissions control response from the model could vary in sign and magnitude. We concluded in our previous study that it cannot be safely assumed that a measure of total change in a resultant concentration like δO_3 from a perturbed input variable properly reflects the change in the photochemical system state which is of primary interest, the $\delta O_3/\delta NO_x$ and $\delta O_3/\delta E_{VOC}$ response. Rather, these control response sensitivities must be evaluated in the model directly.

2. Experiment design and model configurations

CMAQ v4.2 was used in a matrix of sensitivity simulations that treated the model's gas + aerosol + aqueous phase mechanism as a single element, substituting two older mechanisms, CB4 (Gery et al., 1989) and RADM2 (Stockwell et al., 1990), for the larger and newer SAPRC99 (Carter, 2000a, b). Each resulting mechanism perturbation ensemble was run with a full emissions case and with a 50% NO_x control (NO_x50) and a 50% VOC + CO (VOC50) control.

CMAQ was run with horizontal grid spacings of 32 km for the continental US and with one-way nested progeny domains of 8 km for the southeast US and two 2 km domains centered on Atlanta, GA, and on Nashville, TN. A map of these model domains is appended as Fig. 1-Supplement in the supporting material attached to this article along

with a table describing the sensitivity matrix as Table 1-Supplement.

CMAQ's meteorological driver was MM5 (Grell et al., 1994) v3.5 configured with 30 sigma layers and a nominal 38 m surface layer; one-way nested; and with analysis nudging of winds but not temperature or moisture within the planetary boundary layer (PBL) in the 32 and 8 km grids, but no nudging of any kind in the 2 km grids. The Pleim–Xiu land surface model version of MM5, MM5-PX (Xiu and Pleim, 2000), was used in these runs to improve model response to changing soil moisture and vegetation conditions; to partition better the surface energy into sensible and latent heat; and ultimately to provide better estimates of PBL development and final height, and of the temperature and moisture profiles in the PBL.

Emissions for each chemical mechanism were processed from the 1999 National Emissions Inventory (NEI) v1, grown from 1996, and using the Sparse Matrix Operator Kernel Emissions modeling system, (SMOKE) v1.4 with corrected stable plume rise and updated buoyancy algorithms (SMOKE, 2002).

The CMAQ chemical transport model ran with 21 vertical layers compressed from 30 in MM5 but keeping 11 layers in the lowest 1000 m. Chemical mechanism substitutions were carried out in the matrix described above but using in all cases the Models-3 AE3 aerosol module; RADM-type aqueous chemistry and subgrid cloud processes; and the modified Euler backward iterative (MEBI) solver. Advection in the model was by the piecewise parabolic method; horizontal diffusivity by K -theory with K_h grid size dependence; and vertical diffusivity by K -theory with a K_z lower limit of $1.0 \text{ m}^2 \text{ s}^{-1}$.

We report here from a CMAQ modeling series for 4–14 July 1999, a period that includes in the first week a very warm and stable air mass over both Nashville and Atlanta. This was followed by frontal passage at different times in the two progeny domains of two fronts and then a subsiding continental Polar air mass which brought lower maximum temperatures, fair skies, and low dew-points. The first model evaluation day, 4 July, was preceded by four days of model spin up to ensure against undue initialization influence.

3. Observations data sets

In 1999 the continuing Southeastern Aerosol Research and Characterization experiment

(SEARCH) included seven highly enhanced chemistry ground sites for analysis of gas- and aerosol-phase precursors and their photochemical products. Two of the three paired sites were designed to characterize the greater Atlanta, GA, airshed with one site in Atlanta's urban core at Jefferson Street (JST). JST, at 33.78° N latitude, 84.41° W longitude, is directly in the Atlanta industrial/urban core, less than 5 km northwest of the city center, defined as the intersection of I-20 and I-75/85, and near a network of highways and railroad lines. The SEARCH network generates a valuable continuous (365 d yr^{-1}) data set from an extensive array of specialized chemical and physical measurements. Additional information on SEARCH and the JST data sets are at SEARCH (1999). The location and areal surroundings of the CFA site are shown in Fig. 2a-Supplement.

The 1999 Southern Oxidants Study Nashville/Middle Tennessee Ozone Study (SOS99) included comprehensive air quality field experiments on multiple aircraft platforms and at several highly instrumented surface sites in and around the city of Nashville. The chemistry supersite at Cornelia Fort Airpark (CFA) was selected to be at or near the point of maximum O_3 ($\text{P}(\text{O}_3)$) production under predicted average summer advection regimes, 1–2 h downwind from the Nashville urban core, and $\sim 9 \text{ km}$ east and slightly north of the city at 36.19° N latitude, 86.70° W longitude. The site and instrument configuration at CFA are further described in SOS99 (1999). The location and areal surroundings of the CFA site are shown in Fig. 2b-Supplement.

4. Results

4.1. Jefferson Street

Figs. 1a–c show the $[\text{O}_3]$ time series at JST for the three ensemble members SAPRC99, CB4, and RADM2 for all days in the analysis at (a) 32 km, (b) 8 km, and (c) 2 km. (Note the data gap from 6 to 11 July when lightning-induced power disruptions at this site took most instrumentation off-line.) Relative to CB4 and RADM2, SAPRC99 predicted more $[\text{O}_3]$ most every day, often increasing CMAQ's overprediction bias for $[\text{O}_3]$ maxima. SAPRC99's increased peak prediction holds even as the general overprediction recedes at the two finer grid spacings. At the finer grids, 8 km models with all chemistries perform better than the 32 km solutions.

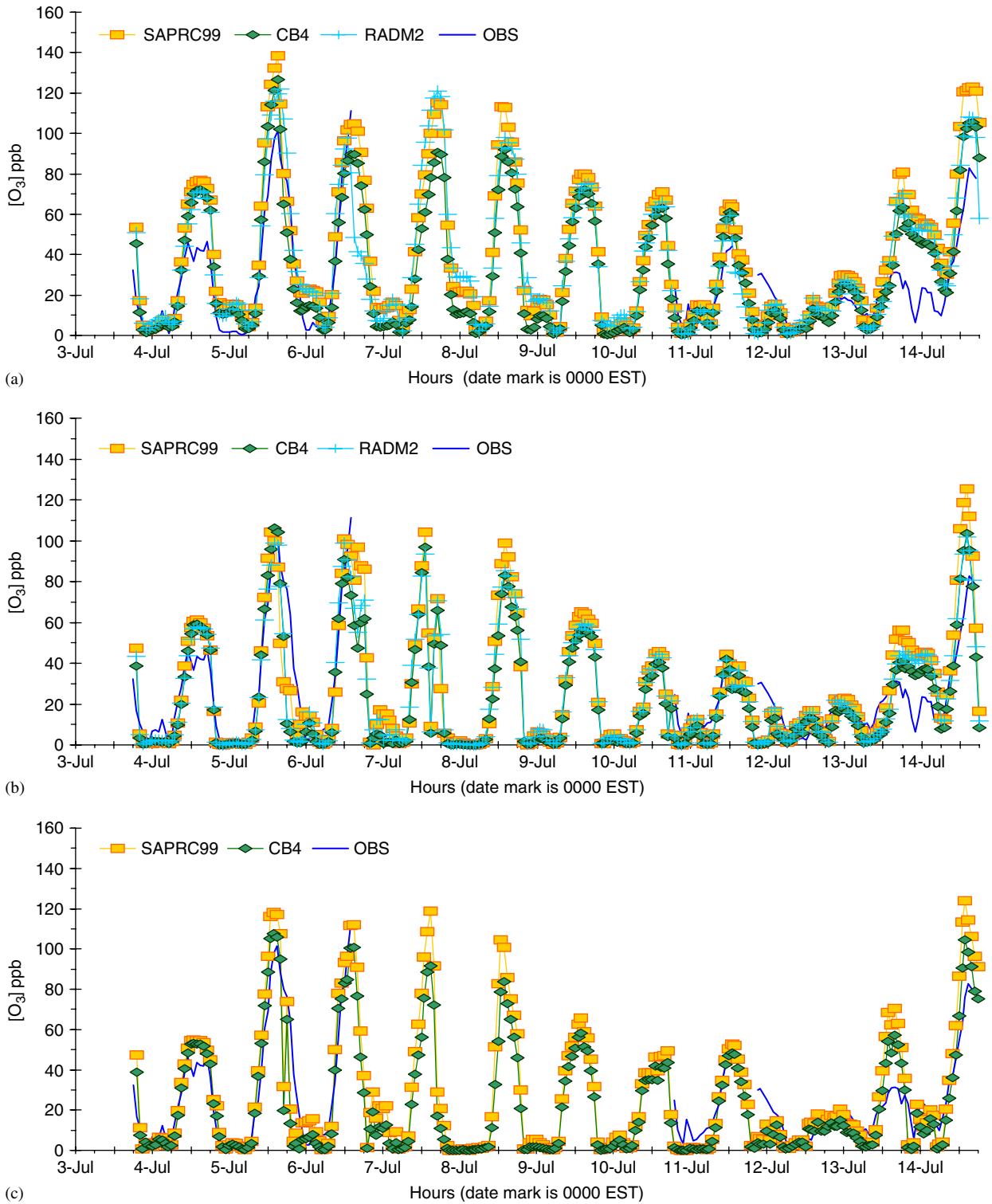


Fig. 1. Time series of 1 h observed and CMAQ-predicted ozone concentration at JST for 3–14 July 1999: CMAQ (a) 32 km, (b) 8 km, (c) 2 km.

Table 1

Maximum 1 h ozone concentrations observed and predicted by CMAQ at 32, 8 and 2 km grid spacings with SAPRC99, CB4, and RADM2 chemistry for site JST in Atlanta

Date	Observed O ₃ (ppb)	Model O ₃ (ppb)	Mod-obs difference (ppb)	Normalized bias(%)	Model O ₃ (ppb)	Mod-obs difference (ppb)	Normalized bias(%)	Model O ₃ (ppb)	Mod-obs difference (ppb)	Normalized bias(%)
SAPRC										
	32 km			8 km			2 km			
4-Jul-99	46.6	76.7	30.1	64.6	61	14.4	30.9	54.9	8.3	17.8
5-Jul-99	101.3	138.5	37.2	36.7	104.2	2.9	2.9	118	16.7	16.5
6-Jul-99	—	104.9	—	—	100.7	—	—	112	—	—
7-Jul-99	—	115.3	—	—	104.2	—	—	118.8	—	—
8-Jul-99	—	113.3	—	—	98.9	—	—	104.4	—	—
9-Jul-99	—	80.0	—	—	65	—	—	65.6	—	—
10-Jul-99	—	71.1	—	—	45.9	—	—	49.2	—	—
11-Jul-99	—	65.1	—	—	44.4	—	—	52.6	—	—
12-Jul-99	16.7	17.8	1.1	6.6	16.9	0.2	1.2	18	1.3	7.8
13-Jul-99	31.3	81.0	49.7	158.8	56.2	24.9	79.6	70.4	39.1	124.9
14-Jul-99	82.8	123.0	40.2	48.6	125.4	42.6	51.4	123.9	41.1	49.6
5 day mean	55.7	87.4	31.7	63.0	72.7	17.0	33.2	77.0	21.3	43.3
CB4										
	32 km			8 km			2 km			
4-Jul-99	46.6	72.1	25.5	54.7	59.0	12.4	26.0	53.1	6.5	13.9
5-Jul-99	101.3	126.5	25.2	24.9	106.3	5.0	5.0	107.5	6.2	6.1
6-Jul-99	—	89.8	—	—	90.8	—	—	100.7	—	—
7-Jul-99	—	90.6	—	—	96.8	—	—	91.6	—	—
8-Jul-99	—	92.0	—	—	83.0	—	—	83.7	—	—
9-Jul-99	—	72.1	—	—	56.1	—	—	58.3	—	—
10-Jul-99	—	63.1	—	—	40.3	—	—	43.5	—	—
11-Jul-99	—	61.0	—	—	42.0	—	—	48.4	—	—
12-Jul-99	16.7	24.7	8.0	48.1	17.0	0.3	1.8	14.9	−1.8	−10.9
13-Jul-99	31.3	63.2	31.9	102.0	41.1	9.8	31.2	57.1	25.8	82.3
14-Jul-99	82.8	105.4	22.6	27.3	103.6	20.8	25.2	104.5	21.7	26.3
5 day mean	55.7	78.4	22.7	51.4	65.4	9.7	17.9	67.4	11.7	23.5
RADM2										
	32 km			8 km						
4-Jul-99	46.6	71.5	24.9	53.5	57.9	11.3	24.2			
5-Jul-99	101.3	122.1	20.8	20.0	98.7	−2.6	−2.6			
6-Jul-99	—	97.6	—	—	98.7	—	—			
7-Jul-99	—	120.9	—	—	93.4	—	—			
8-Jul-99	—	98.1	—	—	85.3	—	—			
9-Jul-99	—	75.0	—	—	59.2	—	—			
10-Jul-99	—	66.1	—	—	44.2	—	—			
11-Jul-99	—	59.4	—	—	41.3	—	—			
12-Jul-99	16.7	25.4	8.7	52.3	22.0	5.3	31.8			
13-Jul-99	31.3	70.2	38.9	124.3	45.8	14.5	46.3			
14-Jul-99	82.8	108.1	25.3	30.5	101.7	18.9	22.9			
5 day mean	55.7	79.5	23.7	56.2	65.2	9.5	24.5			

Ozone concentration difference (model minus observations) in ppb; and percent normalized bias.

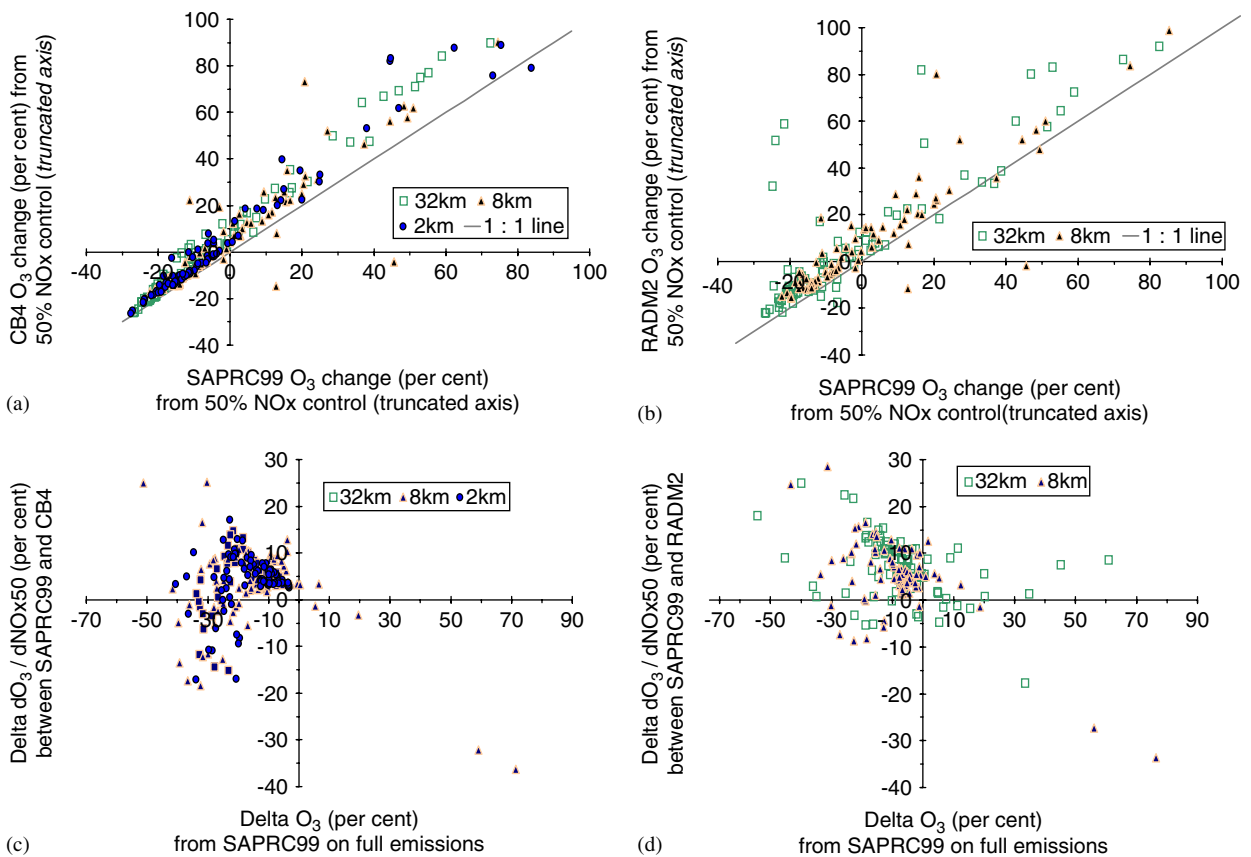


Fig. 2. Model-to-model percent change in ozone from the 50% NO_x control model runs at JST: SAPRC99 chemistry (*x*-axis) vs. (a) CB4 and (b) RADM2. Hours between 1000 and 1700 EST are shown for 4–14 July 1999 with 32, 8 and 2 km grid spacings for CB4 and 32 and 8 km for RADM2. See text for further explanation.

Table 1 shows that the 1-hour normalized bias for peak [O₃] with SAPRC99 fell to 33.2% at 8 km from 63.0% at 32 km; to 17.9% at 8 km from 51.5% at 32 km with CB4; and to 24.5% from 56.2% with RADM2. The 2 km models, however, demonstrate no improvement in 1 h peak [O₃] bias over the 8 km ones with either SAPRC99 or CB4: 43.3% bias with SAPRC99 at 2 km and 23.5% bias with CB4 at 2 km. (Limits on time and computer resources prevented running the RADM2 2 km model for Atlanta.) In addition, the 8 km models performed best of the three for the lowest daytime [O₃] peaks, the 16.7 ppb [O₃] observed on 12 July, for example, and for the overnight [O₃] minima on 5 and 6 July. We believe better performance was obtained with the 8 km models because their smaller grid cell volume more accurately constrains sources emissions, most especially of NO_x. It appears that the 2 km models produce less accurate results because they have inappropriately included or excluded

sources in their even smaller grid cell volumes. This effect at 2 km likely is a complex and ambiguous function of emissions inventory resolution—inventories like the NEI used here are generally built at much higher resolutions—and inaccurate meteorological solutions in small grids.

Figs. 2a and b display the NO_x50 $\delta O_3/\delta NO_x$ $\delta O_3/\delta E_{NO_x}$ response for (a) CB4 and (b) RADM2 with time limited to 1000–1700 EST. JST shows hours of NO_x limitation, when NO_x reductions reduce [O₃], and of NO_x superabundance or radical limitation, when NO_x reductions increased [O₃]. These O₃ benefits and disbenefits were predicted with all chemistries at all grid spacings although there were differences: CB4 and RADM2 predicted less O₃ benefit and more disbenefit than SAPRC99, as well as disbenefits in some hours when SAPRC99 predicted benefits. Points in the northeast quadrant (+, +) above the 1:1 line show O₃ increases from CB4 and RADM2 greater than

from SAPRC99 for hours not benefiting from the NO_x control. Points in the southwest quadrant $(-, -)$ show that CB4 and RADM2 nearly always predicted less O_3 benefit in hours when NO_x control would result in lower O_3 . Work to understand the causes of these distinctions across chemistries is continuing.

Figs. 2c and d combine the δO_3 response in the full emissions base case with the $\delta\text{O}_3/\delta\text{NO}_x$ response in Figs. 2a and 2b. The x -axis for either (c) CB4 or (d) RADM2 represents SAPRC99's O_3 difference relative to the other chemistries in the full emissions case expressed here as percent:

$$\frac{([\text{O}_3]\text{CB4 or RADM2}_{\text{full emissions}} - [\text{O}_3]\text{SAPRC99}_{\text{full emissions}})}{[\text{O}_3]\text{SAPRC99}_{\text{full emissions}}} \times 100\%.$$

The y -axes then represent the percent residual difference between the predicted change in $[\text{O}_3]$ by CB4 and RADM2 relative to the change predicted by SAPRC99 for NO_x50 , i.e. the differential sensitivity to each mechanism in the NO_x50 case

$$\frac{([\text{O}_3]\text{SAPRC99}_{\text{NO}_x50} - [\text{O}_3]\text{SAPRC99}_{\text{full emissions}}) - ([\text{O}_3]\text{CB4 or RADM2}_{\text{NO}_x50} - [\text{O}_3]\text{CB4 or RADM2}_{\text{full emissions}})}{[\text{O}_3]\text{SAPRC99}_{\text{NO}_x50}} \times 100\%.$$

That differential sensitivity varied by more than $\pm 15\%$ with CB4 and by more than $\pm 10\%$ with RADM2, and, importantly, could not be predicted reliably from the model δO_3 response: note, for example, the very large range of response, $\pm \sim 18\%$, in the CB4 2 km control case for hours when CB4 predicted $\sim 25\%$ less O_3 than SAPRC99 with full emissions.

Differences in the model-to-model percent O_3 change at JST from the 50% NO_x control are shown with CB4 (Fig. 2c) and RADM2 (Fig. 2d) vs. the percent O_3 change produced by substituting either CB4 or RADM2 for SAPRC99 in the full emissions base case at 32, 8, and 2 km for CB4, and 32 and 8 km for RADM2. Points clustered in the northwest quadrant $(-, +)$ show that CB4 and RADM2 predicted mostly smaller residual percent changes in O_3 relative to SAPRC99, especially for the 8 and 2 km models. Points in all quadrants suggest that the δO_3 sensitivity response in the base

case (x -axis difference) was not a reliable predictor of sensitivity response in the control case (y -axis differences).

The relations among chemical mechanisms shown here for NO_x50 generally hold for VOC50 at JST, too, where $\delta\text{O}_3/\delta E_{\text{VOC}}$ could not be reliably predicted from the δO_3 either. Figs. 3a and b display the VOC50 $\delta\text{O}_3/\delta E_{\text{VOC}}$ response for (a) CB4 and (b) RADM2. The range of response with VOC control was smaller than that for NO_x control; compare these plots with those in Figs. 2a and b. The VOC control produced no O_3 disbenefits but there were differences among the mechanisms:

mostly smaller O_3 benefits from CB4 than from SAPRC99, and the RADM2 32 km model produced slightly larger benefits than the SAPRC99 32 km one although there was less trend in the 8 km solutions. Points above the 1:1 line in each plot

indicate larger sensitivity response, i.e. greater reduction in $[\text{O}_3]$ with VOC control, from SAPRC99.

Figs. 3c and d depict the model response for VOC50 control analogous to the NO_x control results shown in Figs. 2c and d. CB4 (Fig. 3c) was less sensitive than SAPRC99 but the range was most often within 15%. The RADM2 32 km model (Fig. 3d) was often more sensitive than the corresponding SAPRC99, and the 8 km RADM2 model less sensitive, but the range against the SAPRC99 models for the VOC50 response was largely the same as for CB4. Differential sensitivity to chemical mechanism with VOC50 was similar to that with the NO_x50 control: -5% to $+15\%$ here, compared to $\pm 15\%$ and -10% to $+20\%$ for NO_x control for CB4 and RADM2, respectively. However, as with NO_x , the sensitivity response to the VOC50 could not be reliably predicted from the δO_3 sensitivity response of either mechanism in the full emissions case.

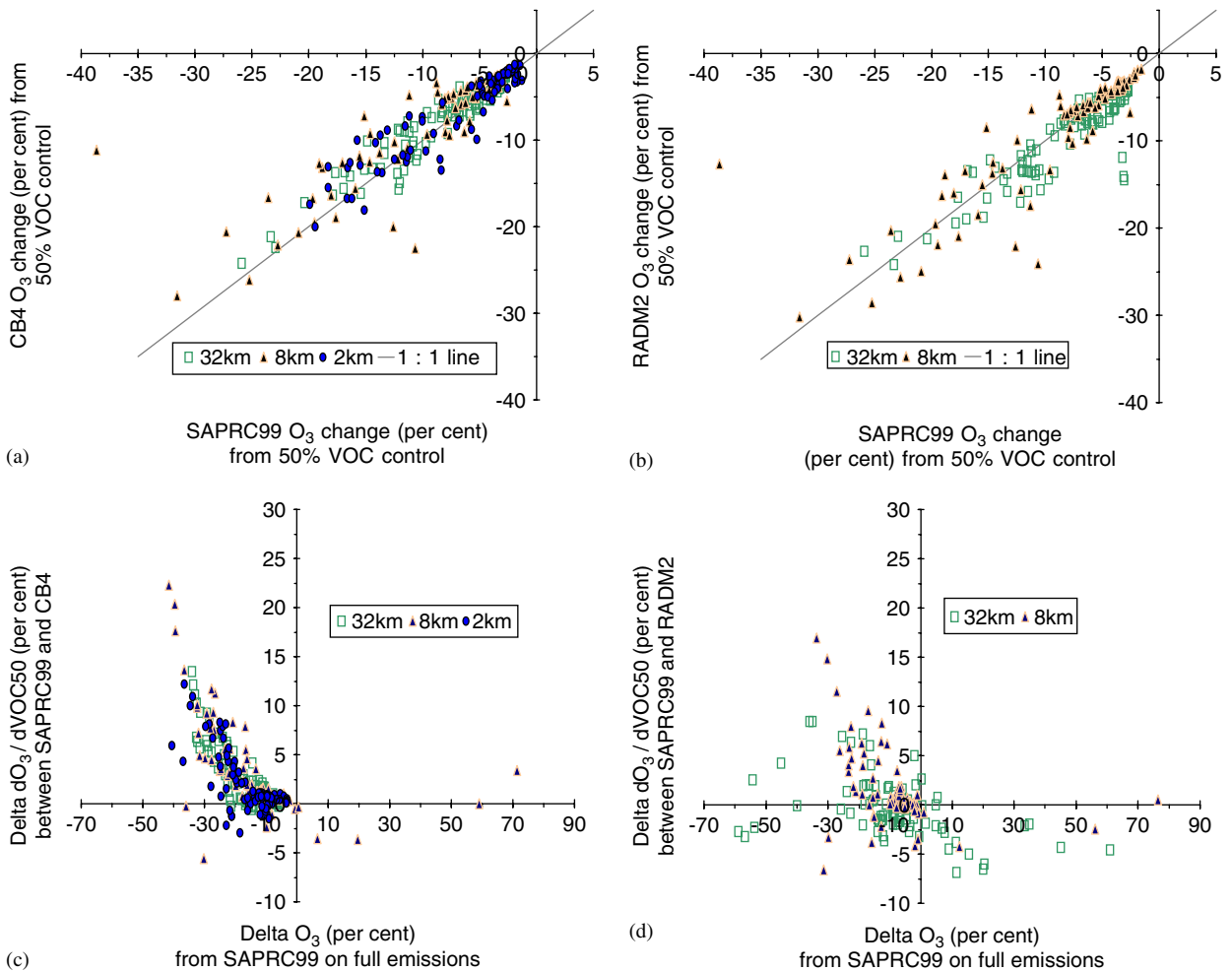


Fig. 3. Model-to-model percent change in ozone from the 50% VOC emissions control runs at JST: SAPRC99 chemistry (*x*-axis) vs. (a) CB4, and (b) RADM2. Hours between 1000 and 1700 EST shown for 4–14 July 1999. 32, 8 and 2 km grid spacings shown for CB4; 32 and 8 km for RADM2. Figs. 3(c) and (d) are read like Figs. 2(c) and (d) above but here for VOC control.

4.2. Cornelia Fort Airpark

Figs. 4a and b show the [O₃] time series at CFA for the three ensemble members SAPRC99, CB4, and RADM2 for all days in the analysis at (a) 32 km and (b) 8 km. (Limits on time and computer resources prevented the running of the 2 km model with CB4 or RADM2 in the Nashville domain.) Unlike at JST, at CFA the 8 km models did not all out-perform the 32 km ones. Only the RADM2 8 km improved from the 32 km solution, and then only for 5 of the 11 days, from a normalized 1 h O₃ peak prediction total mean bias of 15.7 to 10.1%. See Table 2 for additional details. Moreover, the only 2 km model run in the Nashville domain, SAPRC99, showed worse performance than the

8 km or the 32 km ones: 21.5% normalized bias at 2 km, compared with 19.5% at 8 km and 16.0% at 32 km. See Table 2 for additional details.

As at JST, at CFA, SAPRC99 predicted more O₃ than CB4 and RADM2 nearly every day, although RADM2 was nearer to SAPRC99 at CFA than at JST. The substantial O₃ overprediction overnight improved most days at 8 km as did the correlated nighttime under-prediction of total oxidized nitrogen, NO_y (see Figs. 4c and d) (NO_y = NO + NO₂ + NO₃ + 2*N₂O₅ + HONO + HNO₃ + HNO₄ + PAN(s) + other organic nitrates). This O₃ overprediction was not influenced by choice of chemical mechanism, and, as described above, in fact appears to be forced most strongly by a complex interaction of emissions inventory—reflected in the change with

grid spacing—and vertical mixing out of the surface layer. Results from a second sensitivity study we have conducted but do not report here confirmed the dominant role of vertical mixing physics in driving this nighttime bias.

Figs. 5a and b display the NO_x 50 $\delta\text{O}_3/\delta E_{\text{NO}_x}$ response for (a) CB4 and (b) RADM2. Unlike at JST, at CFA, all hours at 32 km and almost all at 8 km showed O_3 benefits from NO_x control, indicating that the urban core site in Atlanta was more strongly radical-limited than was the downwind site at CFA. Points clustered in the southwest

quadrant (–,–) above the 1:1 line in each plot indicate smaller benefits from CB4 and RADM2 relative to SAPRC99 from the NO_x control. At CFA, CB4 and RADM2 were less sensitive than SAPRC99 to NO_x control by as much as a factor of 2. Also unlike at JST, at CFA, compared to SAPRC99, the RADM2 32 and 8 km models demonstrated even less sensitivity to this NO_x control than the corresponding CB4 solutions.

Figs. 5c and d combine the δO_3 response in the full emissions base case with the $\delta\text{O}_3/\delta E_{\text{NO}_x}$ response in Figs. 5a and b for CFA and are read

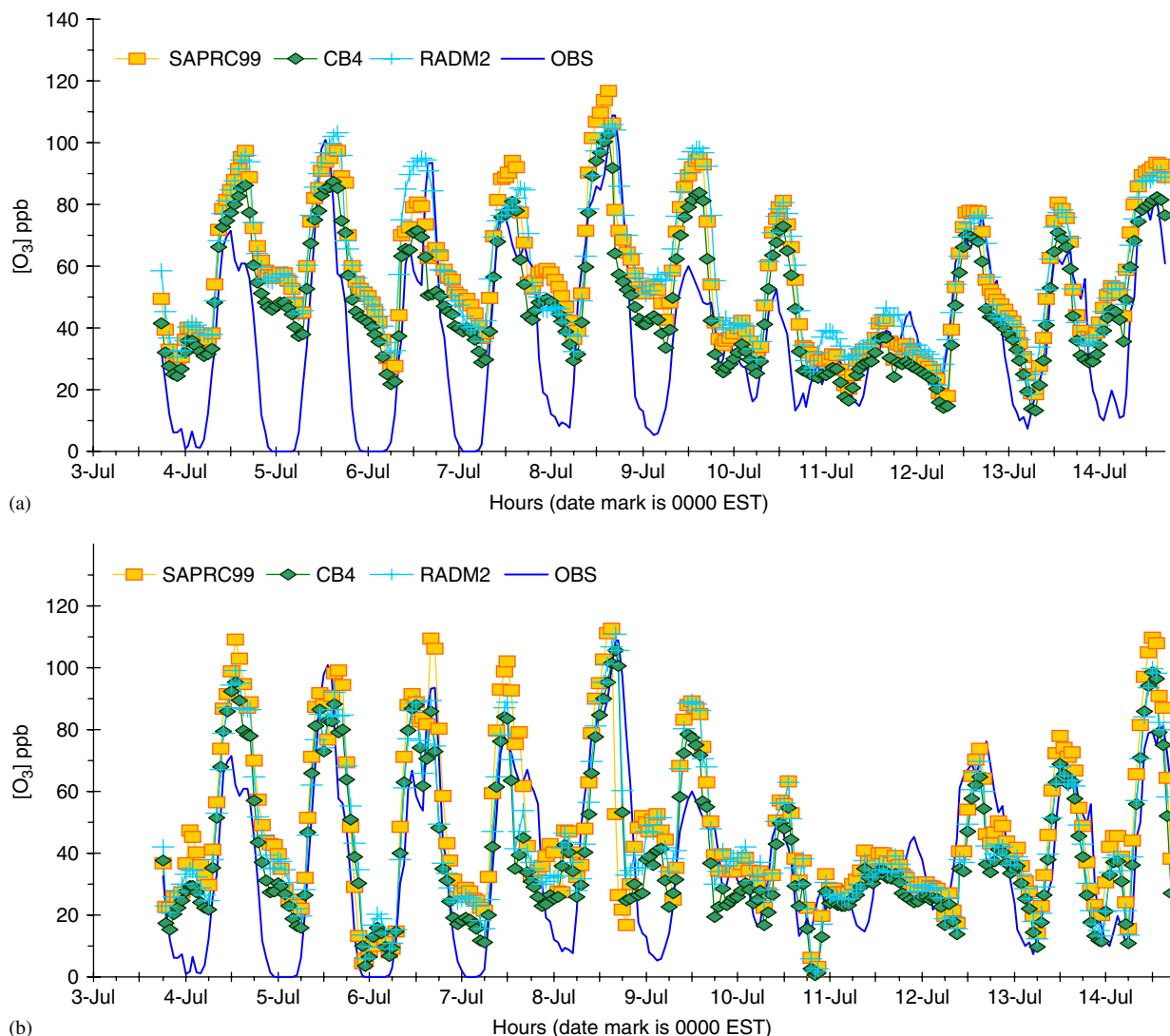


Fig. 4. Time series of observed and CMAQ-predicted hourly ozone concentration at CFA for 3–14 July 1999: CMAQ (a) 32 km and (b) 8 km. (CB4 and RADM2 were not modeled in the 2 km Nashville domain.) Large nighttime over-predictions of ozone on several days are not a function of any particular chemistry and are correlated with underpredictions of NO_y shown in Figs. 4(c) and (d) for the 32 and 8 km models, respectively.

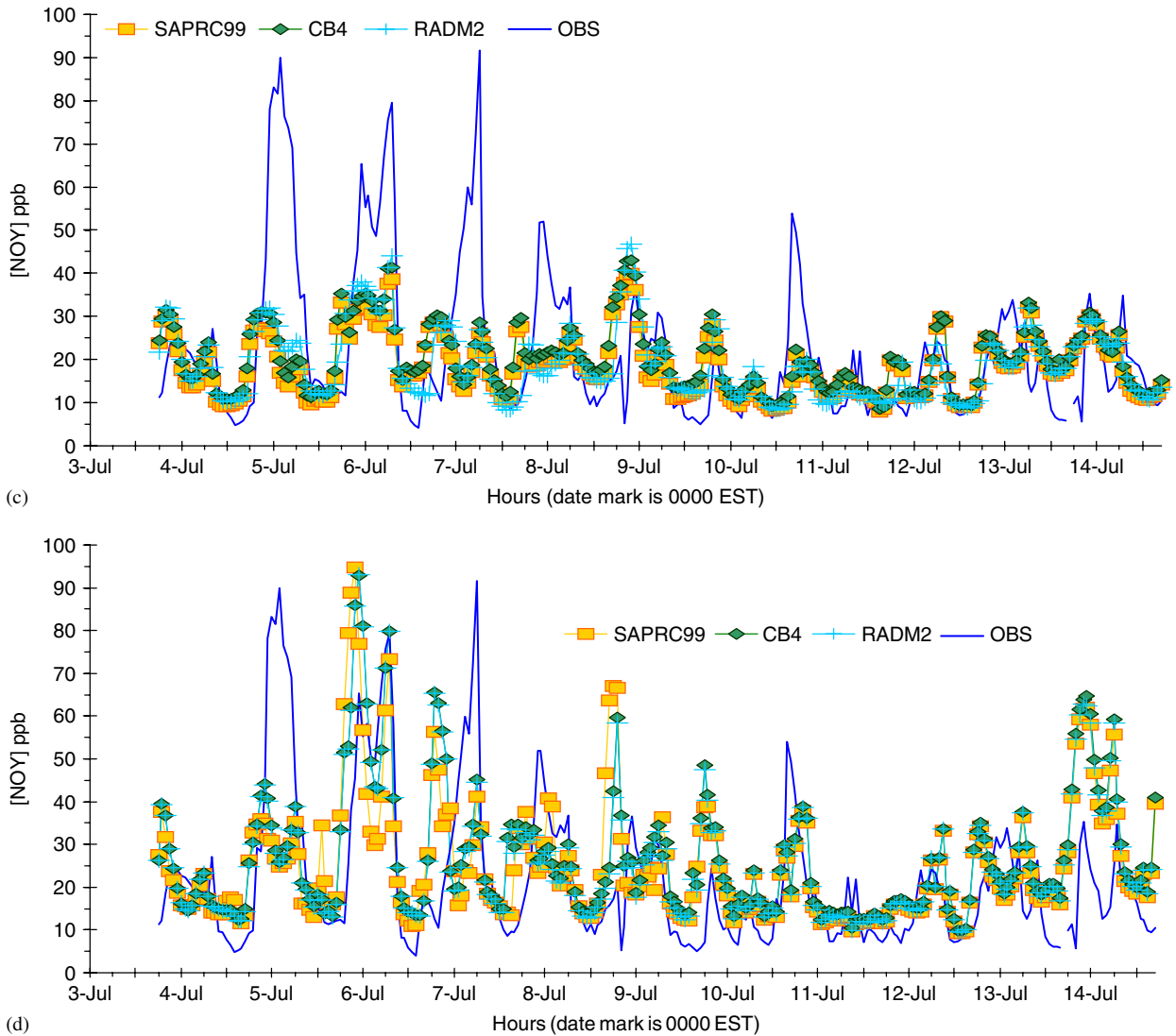


Fig. 4. (Continued)

like Figs. 2c and d for JST above. As at JST, at CFA, points clustered in the northwest quadrant (–, +) show that CB4 and RADM2 predicted mostly smaller residual percent changes in $[O_3]$ relative to SAPRC99. Points in the southeast quadrant (+, –) show hours where SAPRC99 predicted a smaller residual percent change in $[O_3]$ than the other chemistries, chiefly RADM2 32 km. Substituting CB4 for SAPRC99 (Fig. 5c) produced lower O_3 in almost every hour in the full emissions base case at 32 and 8 km. But CB4 was less responsive than SAPRC99 to the NO_x control, and predicted a smaller residual percent change in $[O_3]$, with a differential sensitivity varying in the

range of 2–20%. Substituting RADM2 for SAPRC99 (Fig. 5d) in the full emissions case produced less O_3 at 8 km, but more O_3 76% of the time at 32 km. Like CB4, the RADM2 8 km solution was almost always less responsive than the corresponding SAPRC99 model to this NO_x control, with a differential sensitivity in the range of 2–10%. The RADM2 32 km model was also generally less responsive than the SAPRC99 32 km model to NO_x control even for hours when RADM2 predicted more O_3 in the base case. However, for a small number of hours when RADM2 predicted >10% more O_3 in the base case, RADM2 was also 2–15% more responsive to this NO_x control. Again, as at

Table 2

Maximum 1 h ozone concentrations observed and predicted by CMAQ at 32, 8 and 2 km grid spacings and with SAPRC99, CB4, and RADM2 chemistry for site CFA in Nashville

Date	Observed O ₃ (ppb)	Model O ₃ (ppb)	Mod-obs difference (ppb)	Normalized bias(%)	Model O ₃ (ppb)	Mod-obs difference (ppb)	Normalized bias(%)	Model O ₃ (ppb)	Mod-obs difference (ppb)	Normalized bias(%)
SAPRC										
	32 km			8 km			2 km			
4-Jul-99	71.4	97.4	26.0	36.4	109.1	37.7	52.8	94.2	22.8	31.9
5-Jul-99	100.9	97.9	-3.0	-3.0	99	-1.9	-1.9	99.1	-1.8	-1.8
6-Jul-99	93.5	80.6	-12.9	-13.8	109.5	16.0	17.1	103.4	9.9	10.6
7-Jul-99	77.6	94.1	16.5	21.3	102	24.4	31.4	101.7	24.1	31.1
8-Jul-99	108.8	116.7	7.9	7.3	112.7	3.9	3.6	132.6	23.8	21.9
9-Jul-99	59.9	95.0	35.1	58.6	89.1	29.2	48.7	90.2	30.3	50.6
10-Jul-99	52.2	81.2	29.0	55.6	63.2	11.0	21.1	64.1	11.9	22.8
11-Jul-99	39.0	42.6	3.6	9.2	39.9	0.9	2.3	39.6	0.6	1.5
12-Jul-99	76.2	78.1	1.9	2.5	73.9	-2.3	-3.0	61.2	-15.0	-19.7
13-Jul-99	64.7	80.6	15.9	24.6	78	13.3	20.6	93.3	28.6	44.2
14-Jul-99	81.1	93.4	12.3	15.2	109.8	28.7	35.4	123.2	42.1	51.9
5 day mean	75.0	87.1	12.0	16.0	89.7	14.6	19.5	91.1	16.1	21.5
CB4										
	32 km			8 km						
4-Jul-99	71.4	86.3	14.9	20.8	95.4	24.0	33.6			
5-Jul-99	100.9	87.3	-13.6	-13.4	88.1	-12.8	-12.7			
6-Jul-99	93.5	71.5	-22.0	-23.5	88.0	-5.5	-5.9			
7-Jul-99	77.6	80.8	3.2	4.2	84.0	6.4	8.2			
8-Jul-99	108.8	102.6	-6.2	-5.7	105.7	-3.1	-2.9			
9-Jul-99	59.9	83.7	23.8	39.8	78.4	18.5	30.9			
10-Jul-99	52.2	73.0	20.8	39.9	54.7	2.5	4.7			
11-Jul-99	39.0	37.1	-1.9	-4.8	35.0	-4.0	-10.2			
12-Jul-99	76.2	70.0	-6.2	-8.2	64.7	-11.5	-15.0			
13-Jul-99	64.7	71.0	6.3	9.7	68.8	4.1	6.4			
14-Jul-99	81.1	82.4	1.3	1.6	98.5	17.4	21.5			
5 day mean	75.0	76.9	1.9	2.5	78.3	3.3	4.4			
RADM2										
	32 km			8 km						
4-Jul-99	71.4	95.9	24.5	34.3	99.2	27.8	39.0			
5-Jul-99	100.9	103.3	2.4	2.3	92.0	-8.9	-8.9			
6-Jul-99	93.5	95.0	1.5	1.6	89.6	-3.9	-4.2			
7-Jul-99	77.6	85.2	7.6	9.8	89.0	11.4	14.6			
8-Jul-99	108.8	105.8	-3.0	-2.8	110.7	1.9	1.8			
9-Jul-99	59.9	98.1	38.2	63.8	89.2	29.3	49.0			
10-Jul-99	52.2	80.6	28.4	54.4	83.0	10.8	20.7			
11-Jul-99	39.0	46.3	7.3	18.8	39.0	0.0	0.0			
12-Jul-99	76.2	76.3	0.1	0.2	69.6	-6.6	-8.6			
13-Jul-99	64.7	78.2	13.5	20.8	67.9	3.2	4.9			
14-Jul-99	81.1	90.2	9.1	11.3	99.7	18.6	22.9			
5 day mean	75.0	86.8	11.8	15.7	82.6	7.6	10.1			

Ozone concentration difference (model minus observations) in ppb; and percent normalized bias.

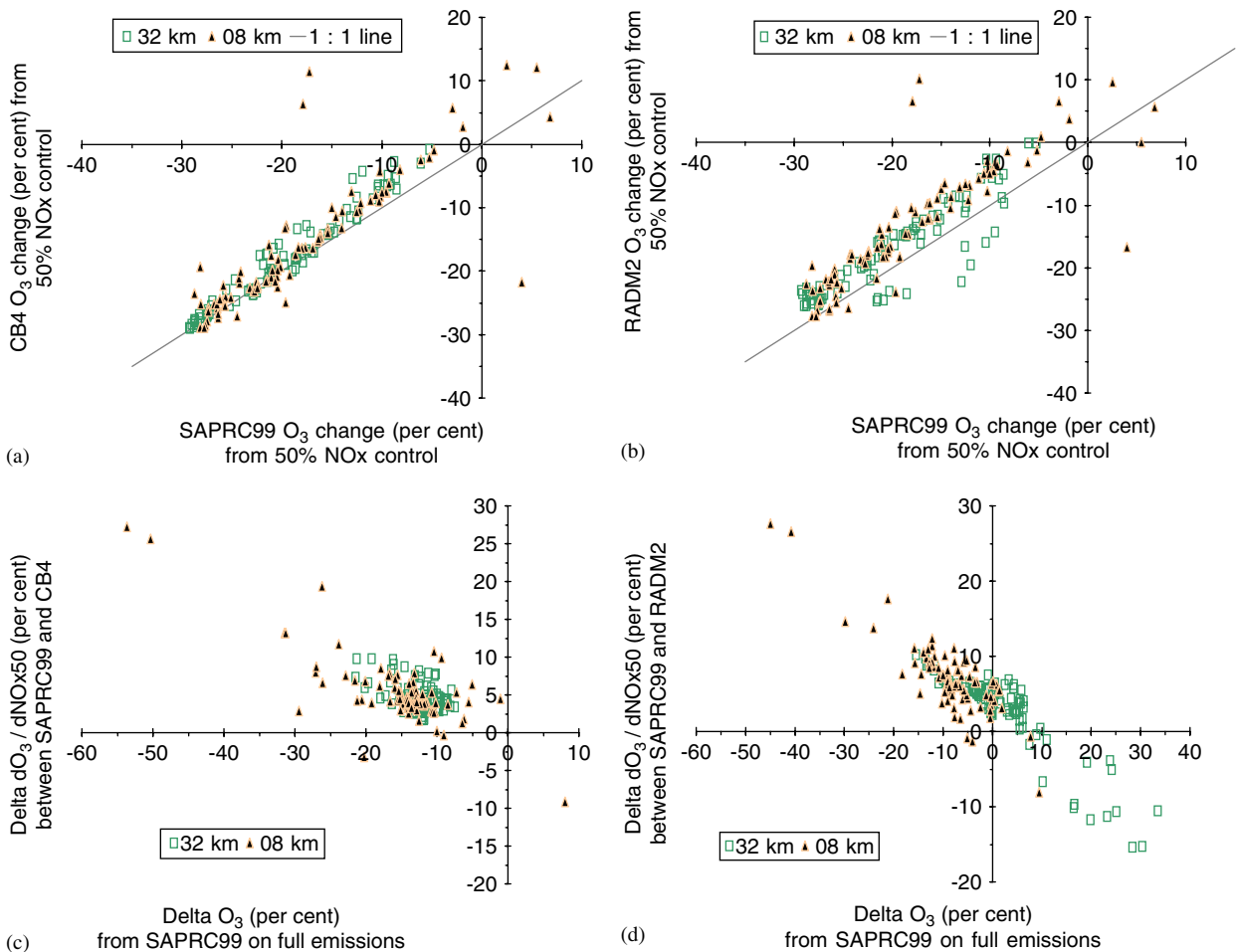


Fig. 5. Model-to-model percent change in ozone from the 50% NO_x control model runs at CFA: SAPRC99 chemistry (*x*-axis) vs. (a) CB4, and (b) RADM2. Hours between 1000 and 1700 EST are shown for 4–14 July 1999: 32 and 8 km grid spacings are shown for all chemistries.

JST, the δO_3 sensitivity response in the base case (*x*-axis difference) at CFA was not a reliable predictor of sensitivity response in the emissions control case.

Model results for the VOC50 control at CFA are depicted in Figs. 6a and b. As at JST, at CFA, the range of response for VOC50 with all mechanisms was markedly smaller than for NO_x control but was smaller at CFA than at JST. O₃ benefits at CFA from CB4 (Fig. 6a) were consistently smaller than those from SAPRC99, as at JST. While the O₃ benefits from the RADM2 8 km model (Fig. 6b) were mostly larger than from the SAPRC99 8 km one, there was less trend at 32 km, precisely the reverse of this grid size dependence at JST.

Figs. 6c and d are the VOC50 analogs for CFA to the combined base case and NO_x control results shown in Figs. 5c and d. The CB4 32 and 8 km

models (Fig. 6c) were less sensitive than their SAPRC99 counterparts, though mostly in a range < 5%, even for hours when CB4 predicted 15–20% less O₃ in the full emissions base case. The RADM2 32 and 8 km models (Fig. 6d) showed no bias in the very small differential sensitivity to SAPRC99: the residual O₃ change was $\pm 3\%$ for most hours irrespective of RADM2's having predicted more or less O₃ in the full emissions base case. The range of differential sensitivity at CFA for the VOC50 control was smaller and showed less trend than at JST, and was smaller than for NO_x control at CFA, also as at JST. And, as at JST, differential sensitivity at CFA with any chemistry to either NO_x or VOC control could not be reliably predicted from the model's δO_3 sensitivity response in the full emissions base case.

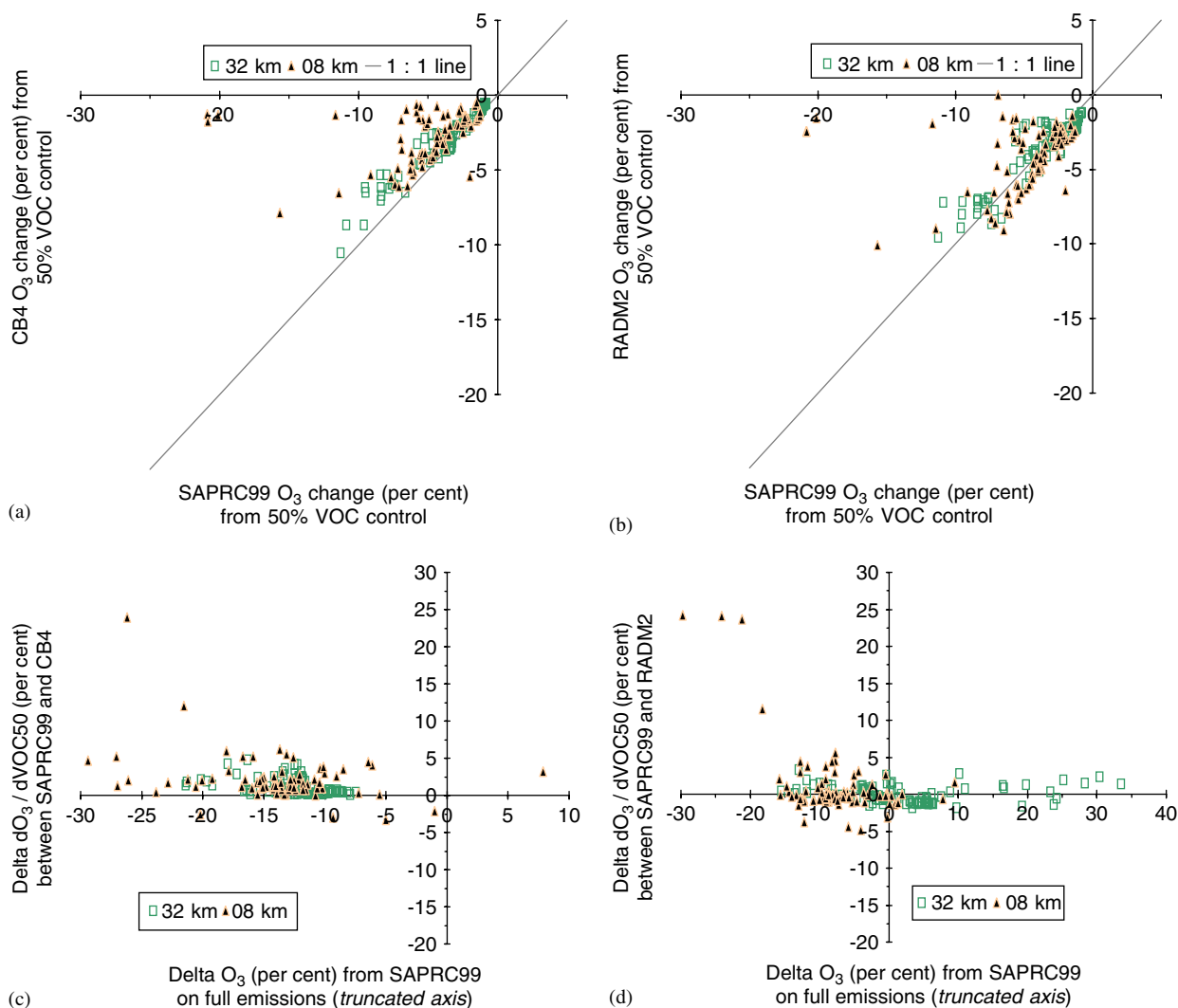


Fig. 6. Same as 5a–d but here for the 50% VOC emissions control. Points above the 1:1 line in each plot indicate a larger sensitivity response from SAPRC99 than from (a) CB4 or (b) RADM2. Model-to-model differences with (c) CB4 and (d) RADM2 from the VOC control combined differences are read like those depicted in Figs. 5c and d for the NO_x control. Note range of response is smaller for VOC control than for NO_x control.

5. Conclusions

5.1. Full emissions cases

Treating CMAQ’s chemical mechanism as a single entity for sensitivity perturbation with full emissions at three grid spacings led to these conclusions from model-to-model and model-to-observations comparisons:

1. SAPRC99 predicted more O₃ than CB4 or RADM2 in most all hours and especially for afternoon maxima at both urban JST and

downwind CFA. These results with CMAQ cohere with those of Jimenez et al. (2003) in their 0-D box model testing of these mechanisms. The RADM2 32 km model alone predicted a substantial number of hours (76%) with more O₃ than SAPRC99, and only at CFA.

2. CB4 predicted the lowest normalized bias for 1 h peak [O₃] in all domains on average and almost every day.
3. The 8 km model performance at JST was better than that from the 32 km models. At CFA only the RADM2 8 km model improved over the 32 km solutions.

Performance at 2 km was worse than that at 8 km at both sites for the chemistries run in each domain.

5.2. Emissions control cases

In the emissions control cases, model-to-model comparisons led to these conclusions:

1. Choice of chemical mechanism altered CMAQ's relative O₃ control response by more than 15% at urban JST and by 5–10% at downwind CFA.
2. SAPRC99 was generally more responsive than CB4 and RADM2 to the 50% NO_x and 50% VOC controls tested here, excepting hours at JST with predicted O₃ disbenefits from the NO_x control.
3. Differential sensitivity to chemical mechanism varied by more than ±10% for NO_x control at JST and CFA, and in a similar range for VOC control at JST; VOC control at the more strongly NO_x-limited CFA site produced a smaller range of differential sensitivity response, most often less than 5%.
4. Even when differential sensitivities were small, neither their sign nor their magnitude could be reliably determined from a model's δO₃ sensitivity response to the chemistry perturbation in the full emissions base case. Hence, model evaluation of sensitivity should also include tests using proposed emissions controls to identify correctly the model's relevant sensitivity response, δO₃/δE_{NO_x} and δO₃/δE_{VOC}.

Disclaimer: The work presented here was performed under the Memorandum of Understanding between the US Environmental Protection Agency (USEPA) and the National Oceanic and Atmospheric Administration (NOAA) of the US Department of Commerce, and under agreement # DW13921548. This work constitutes a contribution to the NOAA Air Quality Program. Although it has been reviewed by USEPA and NOAA and ap-

proved for publication, it does not necessarily reflect the policies or views of either agency.

Appendix A. Supplementary Materials

Supplementary data associated with this article can be found in the online version at doi:10.1016/j.atmosenv.2005.05.055.

References

- Carter, W.P.L., 2000a. Documentation of the SAPRC99 chemical mechanism for VOC reactivity assessment. Final Report to the California Air Resources Board, Contract No. 92-329, and (in part) 95-308. Riverside, CA.
- Carter, W.P.L., 2000b. Implementation of the SAPRC99 chemical mechanism into the Models-3 Framework; <ftp://ftp.cert.ucr.edu/pub/carter/pubs/s99mod3.pdf>.
- Dennis, R.L., Arnold, J.R., Tonnesen, G.S., Li, Y.-H., 1999. A new response surface approach for interpreting Eulerian air quality model sensitivities. *Computer Physics Communications* 117, 99.
- Gery, M., Whitten, G.Z., Killus, J.E., Dodge, M.C., 1989. A photochemical kinetics mechanism for urban and regional scale computer modeling. *Journal of Geophysical Research* 94, 925.
- Grell, A.G., Dudhia, J., Stauffer, D.R., 1994. A description of the fifth-generation Penn State/NCAR mesoscale model (MM5) NCAR Technical Note NCAR/TN-398+STR, National Center for Atmospheric Research, Boulder, CO.
- Jimenez, P., Baldasano, J.M., Dabdub, D., 2003. Comparison of photochemical mechanisms for air quality modeling. *Atmospheric Environment* 37 (30), 4179–4194.
- Russell, A.G., Dennis, R.L., 2000. NARSTO critical review of photochemical models and modeling. *Atmospheric Environment* 34 (12–14), 2283.
- SEARCH, 1999. <http://atmospheric-research.com/studies/SEARCH/>.
- SMOKE, 2002. <http://www.cep.unc.edu/empd/products/smoke/index.shtml>.
- SOS99, 1999. <http://www.al.noaa.gov/WWHD/pubdocs/SOS/sos99.groundsites.html>.
- Stockwell, W.R., Middleton, P., Chang, J.S., Tang, X., 1990. The second generation Regional Acid Deposition Model chemical mechanism for regional air quality modeling. *Journal of Geophysical Research* 95, 16343.
- Xiu, A., Pleim, J.E., 2000. Development of a land surface model. Part II: application in a mesoscale meteorology model. *Journal of Applied Meteorology* 40, 192.